

Distributed Dynamic Associative Memory via Online Convex Optimization

Bowen Wang, Matteo Zecchin, *Member, IEEE*, and Osvaldo Simeone, *Fellow, IEEE*

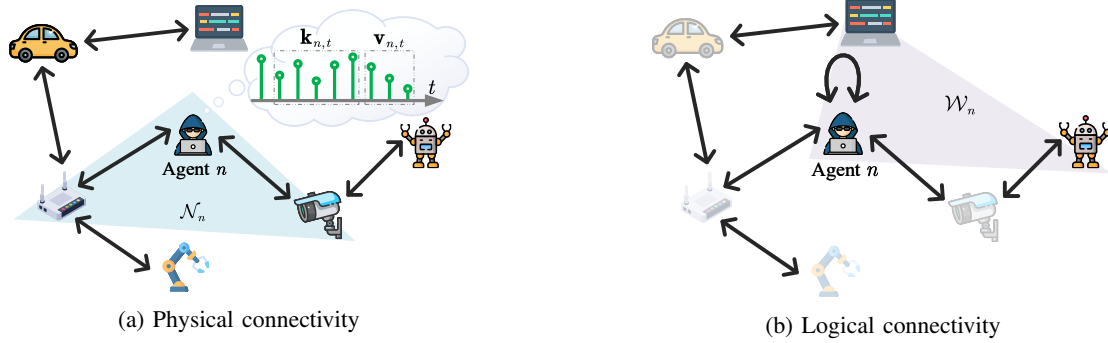


Fig. 1. (a) In a distributed dynamic associative memory (DDAM) system, each agent maintains a local memory, and corresponding AM mechanism, by processing local, streaming, data, as well as by interacting with other agents over a physical network. Each agent n collects streaming data in the form of key $\mathbf{k}_{n,t}$ and value $\mathbf{v}_{n,t}$ over discrete time $t = 1, 2, \dots, T$. The blue region represents the subset \mathcal{N}_n of physical neighbors that can directly exchange information with agent n over the network. (b) The goal of DDAM is for the memory at each agent not only to recall associations from its own data, but also from a subset of other agents. The purple region in the figure represents the logical subset \mathcal{W}_n of agents whose data is relevant for agent n . The nodes in subset \mathcal{W}_n may not be physical neighbors of agent n . Through inter-agent communication over the physical network, DDAM aims at recalling information from both local and logically related agents in an online fashion.

Abstract—An associative memory (AM) enables cue–response recall, and it has recently been recognized as a key mechanism underlying modern neural architectures such as Transformers. In this work, we introduce the concept of distributed dynamic associative memory (DDAM), which extends classical AM to settings with multiple agents and time-varying data streams. In DDAM, each agent maintains a local AM that must not only store its own associations but also selectively memorize information from other agents based on a specified interest matrix. To address this problem, we propose a novel tree-based distributed online gradient descent algorithm, termed DDAM-TOGD, which enables each agent to update its memory on the fly via inter-agent communication over designated routing trees. We derive rigorous performance guarantees for DDAM-TOGD, proving sublinear static regret in stationary environments and a path-length dependent dynamic regret bound in non-stationary environments. These theoretical results provide insights into how communication delays and network structure impact performance. Building on the regret analysis, we further introduce a combinatorial tree design strategy that optimizes the routing trees to minimize communication delays, thereby improving regret bounds. Numerical experiments demonstrate that the proposed DDAM-TOGD framework achieves superior accuracy and robustness compared to representative online learning baselines such as consensus-based distributed optimization, confirming the benefits of the proposed approach in dynamic, distributed environments.

Index Terms—Associative memory, distributed optimization, online convex optimization, regret analysis.

An earlier version of this paper was submitted in part at the IEEE International Conference on Acoustics, Speech, and Signal Processing (ICASSP), 4–8 May, Barcelona, Spain, 2026 [1].

This work was partially supported by the Open Fellowships of the EPSRC (EP/W024101/1) and by the EPSRC project (EP/X011852/1).

The authors are with the King’s Communications, Learning and Information Processing (KCLIP) Lab, Centre for Intelligent Information Processing Systems, Department of Engineering, King’s College London, London WC2R 2LS, U.K. (e-mail: {bowen.wang, matteo.l.zecchin, osvaldo.simeone}@kcl.ac.uk).

I. INTRODUCTION

A. Context and Motivation

An associative memory (AM), originally rooted in psychology and cognitive science, refers to the ability to store cue–response pairs and to recall the corresponding response when a cue is presented [2]. For instance, seeing an image of a banana can evoke its distinctive smell and taste; hearing a person’s name can bring to mind their appearance, habits, or personality. This principle of cue-based recall has inspired developments across neuroscience, signal processing, and machine learning.

Most recently, modern sequence models, notably the Transformer [3], have been interpreted as implementing an AM mechanism [4]–[6]. The attention operation in Transformers performs content-based retrieval of information, effectively recalling relevant *responses* (*values*) based on presented *cues* (*keys*). In fact, inference in such models can be viewed as a form of online memory building and retrieval, which can be formalized via *online convex optimization* (OCO) [7], [8].

However, existing AM mechanisms are *centralized*: all information is processed and stored by a single model or agent. In contrast, many real-world applications operate in inherently *distributed* environments. As illustrated in Fig. 1, examples include sensor networks, internet-of-things (IoT) systems, and cellular wireless networks, where multiple agents, such as devices, sensors, or infrastructure nodes, observe only local data [9]–[12]. In such networks, an agent could benefit from recalling associations not only from its own data but also from other agents’ data relevant to its task. For instance, in an IoT-based surveillance scenario with multiple camera sensors, each camera may capture a different viewpoint of the same scene or object. By sharing information across cameras, the AM at one

camera could recall information about the same object from multiple perspectives, improving tasks such as recognition and tracking.

In multi-agent networks, such as the aforementioned communication networks, data often arrive as a continuous, non-stationary stream [13]. Over time, the underlying data distribution and target associations may evolve. This scenario is common in tasks including traffic analysis, in which data statistics vary as a function of the time of day and/or of the season [14]. A static AM may become outdated as new data arrive or as the environment changes. Therefore, it is important to develop a dynamic associative memory that can adapt online to non-stationary data, updating stored associations, retrieving new relevant information, and forgetting outdated associations as needed.

In summary, many practical settings demand an online, distributed AM that enables multiple agents to jointly and adaptively memorize relevant information over time. Motivated by these considerations, this paper focuses on the study of *distributed dynamic associative memory* (DDAM). Our goal is to bridge the gap between classical centralized AM mechanisms and the requirements of distributed, time-varying environments. In the following, we outline the state of the art and then summarize our contributions.

B. State of the Art

Associative Memory (AM): Early studies of AM trace back to the Hopfield network [15], where memory retrieval is modeled as the minimization of an energy function toward attractor states representing stored patterns. Building upon this formulation, subsequent works proposed dense [16] and continuous [17] Hopfield networks, which generalize the energy function and improve the memory capacity. These models [15]–[17] constitute a family of energy-based AMs, where inference corresponds to energy minimization. More recently, Transformers [3] and related sequence models have been interpreted as AM mechanisms [18]–[22], where the attention operation performs content-based retrieval from representations [4]–[6]. From this viewpoint, inference in such models can be seen as solving an online optimization problem [7], [8] for the storage and retrieval of information.

Online Convex Optimization (OCO): OCO [7], [8] is performed over a sequence of consecutive rounds, where at each round a learner selects a decision. After the decision is made, a cost function is revealed and the learner incurs a corresponding loss. The learner then updates its parameters based on the observed loss to improve subsequent performance. This procedure may model AM [4]–[6], where cues evoke responses that are iteratively corrected through feedback. In OCO, the performance metric is the *regret* [7], [8], which can be categorized as either static or dynamic.

The *static regret* [7], [8], [23] measures the difference between the cumulative loss incurred by the algorithm and that of the best fixed decision in hindsight. In contrast, the *dynamic regret* [23]–[26] quantifies the performance gap with respect to a time-varying comparator sequence, capturing the algorithm’s adaptability to non-stationary environments. To minimize regret, two of the most widely used algorithms

are *online gradient descent* (OGD) [23] and *follow-the-regularized-leader* (FTRL) [7], [8]. Compared with FTRL, OGD is computationally simpler and faster, as it updates the model using only the current gradient without storing past information.

Distributed learning: Distributed learning has been an active research direction for decades. Depending on the learning objective, it can be broadly categorized into single-task learning and multi-task learning [27]. Within single-task distributed learning, it can be further divided into parameter-server-based and fully decentralized paradigms [27]. In the parameter-server-based settings, the most well-known paradigm is federated learning [28], where each agent optimizes a local objective using its own data and periodically aggregates model updates to obtain a global model. In contrast, fully decentralized learning is based on inter-agent message passing [29]. Specifically, in consensus-based distributed learning [30], agents exchange information only with their neighbors and iteratively update to reach an agreement on a common model. In multi-task distributed learning formulations, the problem is to learn multiple heterogeneous, but generally related tasks distributed over agents [31]. Existing approaches either infer task correlations from data-driven similarity measures [32] or define them explicitly through spatial or geographical adjacency [33].

C. Main Contributions

In this paper, we introduce the problem of DDAM and propose a novel DDAM protocol with both static and dynamic regret guarantees. The main contributions of this paper are summarized as follows.

- **Formulation of DDAM:** As illustrated in Fig. 1, we formalize the DDAM problem, in which N agents collaboratively optimize their local associative memories in an online fashion. Each agent n processes its own stream of data, and aims to memorize not only its local input–output associations but also information from a selected subset of other agents.
- **Novel protocol – DDAM-TOGD:** We propose *DDAM via tree-based OGD* (DDAM-TOGD) as an efficient solution to the DDAM problem. In DDAM-TOGD, each agent runs an instance of OGD that is augmented with network communication. Specifically, every agent periodically broadcasts its memory parameters along a spanning tree that connects to all agents whose data it needs. Those agents compute gradient feedback using their local data and send the gradients back along the reverse path.
- **Regret analysis:** We rigorously analyze the performance of DDAM-TOGD in terms of regret. Specifically, we prove that in static environments, DDAM-TOGD achieves sublinear static regret. Hence, each agent’s memory asymptotically approaches the best *fixed memory* in hindsight. Moreover, for dynamic environments, we prove a dynamic regret bound that scales with the path-length of the time-varying optimal memories. Accordingly, if the underlying optimal association for each agent changes slowly over time (small path-length), DDAM-TOGD can track these changes closely and incur low regret. In

contrast, if the environment changes more rapidly, the regret grows accordingly, which is inevitable in the worst case.

- **Communication-efficient tree design:** The regret analysis of DDAM-TOGD provides insights into how communication delays affect performance. Building on this insight, we propose a combinatorial optimization approach to design the communication trees for each agent.
- **Experimental validation:** We validate the proposed DDAM framework through extensive numerical experiments. We compare against existing online optimization baselines such as independent (non-cooperative) online learners and consensus-based distributed OGD. DDAM-TOGD is demonstrated to achieve lower regret and error rates across various scenarios, including both stationary and dynamic settings.

D. Organization

The remainder of this paper is organized as follows. Sec. II defines the problem formulation. Sec. III presents the state-of-the-art protocols. Sec. IV proposes the DDAM protocol and a communication-efficient tree design. Sec. V provides a proof sketch of the regret guarantees. Finally, Sec. VI illustrates the experimental setting and results, and Sec. VII concludes the paper.

II. PROBLEM STATEMENT

We study DDAM in a setting with networked N agents. As shown in Fig. 1, each agent n processes a stream of *keys* $\mathbf{k}_{n,t} \in \mathbb{R}^{d_k}$ and *values* $\mathbf{v}_{n,t} \in \mathbb{R}^{d_v}$, which evolve over discrete time $t = 1, 2, \dots, T$. For example, the key $\mathbf{k}_{n,t}$ may consist of context samples in a time series, and the value $\mathbf{v}_{n,t}$ may include future samples of the same time series. Alternatively, key $\mathbf{k}_{n,t}$ and value $\mathbf{v}_{n,t}$ may represent embeddings of streaming tokens for multi-modal memory recall tasks [4]–[6]. The goal is to dynamically optimize an AM mechanism at each n -th agent, ensuring that at each time t , agent n not only recalls its past data $\{\mathbf{k}_{n,t'}, \mathbf{v}_{n,t'}\}_{t'=1}^t$, but also data $\{\mathbf{k}_{m,t'}, \mathbf{v}_{m,t'}\}_{t'=1}^t$ that is processed by a subset of other agents $m \neq n$.

A. Setting

Denote as $\mathbf{X}_{n,t} \in \mathcal{X}$ the parameters of the AM mechanism maintained at agent n at time t , where \mathcal{X} is the design domain for parameter $\mathbf{X}_{n,t}$. For example, for a *linear AM*, the parameters $\mathbf{X}_{n,t}$ correspond to a $d_v \times d_k$ matrix, and the AM mechanism returns the estimated value $\mathbf{X}_{n,t} \mathbf{k}_{n,t}$ for the input key $\mathbf{k}_{n,t}$. More generally, a linear AM mechanism may operate in a $d_{k'}$ -dimensional space via a $d_v \times d_{k'}$ matrix $\mathbf{X}_{n,t}$ returning the output vector $\mathbf{X}_{n,t} \phi(\mathbf{k}_{n,t})$, where $\phi(\cdot) \in \mathbb{R}^{d_{k'}}$ is a non-linear feature-extraction function.

The AM mechanism at agent n can be generally queried to recall data $(\mathbf{k}_{m,t}, \mathbf{v}_{m,t})$ of any agent m , including itself. The performance of AM $\mathbf{X}_{n,t}$ at agent n in recalling the data $(\mathbf{k}_{m,t}, \mathbf{v}_{m,t})$ of agent m is measured by a cost function $f_{m,t}(\mathbf{X}_{n,t})$. Commonly used memory retrieval cost functions for linear AM are of the form

$$f_{m,t}(\mathbf{X}_{n,t}) = \ell(\mathbf{X}_{n,t}, \mathbf{k}_{m,t}, \mathbf{v}_{m,t}) + \mathcal{R}(\mathbf{X}_{n,t}), \quad (1)$$

TABLE I
MEMORY RETRIEVAL COST FUNCTIONS $f(\mathbf{X})$ OF THE FORM (1) FOR DIFFERENT VARIANTS OF LINEAR ATTENTION [19], WHERE \mathbf{X} REPRESENTS THE MEMORY MATRIX, \mathbf{k} IS THE KEY VECTOR, AND \mathbf{v} IS THE CORRESPONDING VALUE VECTOR. (ψ IS A GATING VECTOR WITH BINARY ENTRIES THAT IS INDEPENDENT OF \mathbf{X} , AND $\phi(\cdot)$ DENOTES A FEATURE-EXTRACTION FUNCTION.)

Model	$\ell(\mathbf{X}, \mathbf{k}, \mathbf{v})$	$\mathcal{R}(\mathbf{X})$
Linear attention [19]	$-\langle \mathbf{X} \mathbf{k}, \mathbf{v} \rangle$	—
Gated linear attention [20]	$-\langle \mathbf{X} \mathbf{k}, \mathbf{v} \rangle$	$\frac{1}{2} \ \text{diag}(\sqrt{1 - \psi}) \mathbf{X}\ _F^2$
DeltaNet [21]	$\frac{1}{2} \ \mathbf{X} \mathbf{k} - \mathbf{v}\ ^2$	—
Softmax attention w/o norm	$-\langle \mathbf{X} \phi(\mathbf{k}), \mathbf{v} \rangle$	—
Softmax attention w/ norm [3]	$-\langle \mathbf{X} \phi(\mathbf{k}), \mathbf{v} \rangle$	$\frac{1}{2} \ \mathbf{X}\ _F^2$
Gated softmax attention [22]	$-\langle \mathbf{X} \phi(\mathbf{k}), \mathbf{v} \rangle$	$\frac{1}{2} \ \text{diag}(\sqrt{1 - \psi}) \mathbf{X}\ _F^2$

where $\ell(\mathbf{X}_{m,t}, \mathbf{k}_{m,t}, \mathbf{v}_{m,t})$ is a cost function comparing the true value $\mathbf{v}_{m,t}$ with the value estimated based on memory $\mathbf{X}_{m,t}$, and $\mathcal{R}(\mathbf{X}_{m,t})$ is a regularization function. Examples of cost functions for linear AM are summarized in Table I.

The overall retrieval cost for agent n weights the cost $f_{m,t}(\mathbf{X}_{n,t})$ with respect to the information from agent m through the parameter $0 \leq w_{n,m} \leq 1$, with $\sum_{m=1}^N w_{n,m} = 1$. Accordingly, the weight $w_{n,m}$ dictates the relevance of the data streamed at agent n itself. Mathematically, the cumulative cost function at time T for agent n is given by

$$\mathcal{L}_n^T(\mathbf{X}_n^T) = \sum_{t=1}^T \sum_{m \in \mathcal{W}_n} w_{n,m} f_{m,t}(\mathbf{X}_{n,t}), \quad (2)$$

where $\mathbf{X}_n^T = \{\mathbf{X}_{n,t}\}_{t=1}^T$, and $\mathcal{W}_n = \{m \in \mathcal{N} | w_{n,m} > 0\}$ denotes the set of agents m whose data is relevant to agent n , i.e., those with nonzero weights $w_{n,m}$. The logical weights defining the cumulative cost (2) are collected into the row stochastic matrix \mathbf{W} with $[\mathbf{W}]_{n,m} = w_{n,m}$, which is assumed to be known at all agents (see Fig. 1(b)).

Since the data $(\mathbf{k}_{m,t}, \mathbf{v}_{m,t})$ are only available to agent m , the cost function $f_{m,t}(\cdot)$ can only be evaluated by agent m . Therefore, in order to optimize the cost function (2), as seen in Fig. 1(a), agent n must generally communicate with other agents, unless the agent n only recalls local data, i.e., $w_{n,n} = 1$. To enable inter-agent communication, agents interact over an *undirected graph* $\mathcal{G} = (\mathcal{N}, \mathcal{E})$, where $\mathcal{N} = \{1, 2, \dots, N\}$ is the set of agent indices, and $\mathcal{E} \subseteq \mathcal{N} \times \mathcal{N}$ is a collection of inter-agent links (m, n) , indicating that agents n and m can communicate. We let $\mathcal{N}_n = \{m \in \mathcal{N} : (m, n) \in \mathcal{E}\}$ denotes the set of neighbors of agent n . Note that the set of edges \mathcal{E} represents the physical connectivity of the agents (see Fig. 1(a)), while the weight matrix \mathbf{W} reflects the logical relationships among the performance requirements of different agents (see Fig. 1(b)).

B. Problem Definition

In this paper, we adopt a worst-case design approach, where optimality is evaluated with respect to the optimal solutions corresponding to the given sequences of keys and values observed by the agents. Specifically, we investigate the following design objectives:

- **Static regret:** The static regret is defined as the difference between the cumulative loss incurred by an online algorithm and the cumulative loss of the best fixed solutions

$\{\mathbf{U}_n^*\}_{n \in \mathcal{N}}$ in hindsight. The optimal solution for each agent n is given by

$$\mathbf{U}_n^* = \arg \min_{\mathbf{U} \in \mathcal{X}} \mathcal{L}_n^T(\mathbf{U}), \quad (3)$$

which is generally different across agents. Summing over the N agents, the static regret is defined as

$$\text{S-Reg}(T) = \sum_{n \in \mathcal{N}} (\mathcal{L}_n^T(\mathbf{X}_n^T) - \mathcal{L}_n^T(\mathbf{U}_n^*)). \quad (4)$$

The static regret is relevant in stationary environments, for which there exists a single AM mechanism that can memorize well enough all data streamed within the time horizon T .

- **Dynamic regret:** The static regret is not an appropriate design criterion for changing environments, in which no single AM mechanism can retrieve data with sufficient accuracy over the entire time horizon of T time steps. In this case, the static regret in (4) may be negative, since there may exist online AM policies that outperform the best static solution in (3), even if the latter has access in hindsight to the entire data to be memorized.

To address this limitation, we also study the dynamic regret [23]–[26], in which the regret is evaluated against any sequence of changing AM mechanisms $\mathbf{U}_n^T = \{\mathbf{U}_{n,t}\}_{t=1}^T$, with $\mathbf{U}_{n,t} \in \mathcal{X}$ for all t and $n \in \mathcal{N}$, as

$$\text{D-Reg}(T) = \sum_{n \in \mathcal{N}} (\mathcal{L}_n^T(\mathbf{X}_n^T) - \mathcal{L}_n^T(\mathbf{U}_n^T)). \quad (5)$$

Note that static regret (4) can be viewed as a special form of dynamic regret (5) by setting the reference AM mechanism $\mathbf{U}_{n,t}$ as the fixed best solution in hindsight, i.e., $\mathbf{U}_{n,t} = \mathbf{U}_n^*$ for all time step t .

C. Technical Assumptions

The analysis in this paper assumes the following standard conditions, which have also been adopted in, e.g., [23]–[26].

Assumption 1. The design domain $\mathcal{X} \subseteq \mathbb{R}^d$ is closed, convex, and it includes the origin, i.e., $\mathbf{0} \in \mathcal{X}$. Furthermore, the cost function $f_{n,t}(\mathbf{X}_{n,t})$ is convex within the domain \mathcal{X} at every time step t for all $n \in \mathcal{N}$.

Note that all cost functions listed in Table I satisfy this assumption with \mathcal{X} being the space of all matrices of suitable dimensions.

Assumption 2. The diameter of the design domain \mathcal{X} is upper bounded by $B < \infty$, i.e., $\|\mathbf{X} - \mathbf{Y}\| \leq B$ for all $\mathbf{X}, \mathbf{Y} \in \mathcal{X}$.

Based on Assumptions 1 and 2, it follows that the norm of the AM parameters \mathbf{X} is bounded as $\|\mathbf{X}\|^2 \leq B$.

Assumption 3. For every time step t and any $\mathbf{X} \in \mathcal{X}$, the gradient of the cost function $f_{n,t}(\cdot)$ is bounded in Euclidean norm by a constant G_n with $0 < G_n < \infty$, i.e., $\|\nabla f_{n,t}(\mathbf{X})\| \leq G_n$.

III. CONVENTIONAL PROTOCOLS

In this section, we review conventional solutions that can be leveraged to design DDAM protocols. Specifically, we

first study the ideal case in which every agent has access to full information, i.e., to all functions $\{f_{n,t}(\cdot)\}_{n \in \mathcal{N}}$. Then, we consider the special case of the DDAM problem introduced in Sec. II, in which agents assign the same weight to the data of all agents, i.e., $\mathbf{W} = \mathbf{1}\mathbf{1}^T/N$. In this setting, one can impose without loss of optimality that all agents share identical AM parameters, so that distributed consensus protocols [34] provide suitable solutions to the DDAM problem.

A. Full-Information DDAM

For reference, we consider first an ideal full-information setting in which all agents have direct access to the data streams of all agents. In this case, each agent n can evaluate the complete set of cost functions $\{f_{n,t}(\cdot)\}_{n \in \mathcal{N}}$, and thus the cumulative cost (2), at every time step t .

In this idealized setting, the problem of minimizing the static or dynamic regret can be addressed via OGD [7], [8], [23]. Specifically, OGD yields the update [7], [8], [23]

$$\mathbf{X}_{n,t+1} = \Pi_{\mathcal{X}} \left[\mathbf{X}_{n,t} - \eta_n \sum_{m \in \mathcal{W}_n} w_{n,m} \nabla f_{m,t}(\mathbf{X}_{n,t}) \right], \quad (6)$$

where $\Pi_{\mathcal{X}}[\cdot]$ denotes the projection onto the design set \mathcal{X} , and η_n is the learning rate.

The regret properties of OGD follow directly from standard results [7].

Theorem 1. Under Assumptions 1–3, OGD attains the dynamic regret

$$\text{D-Reg}(T) \leq \sum_{n \in \mathcal{N}} \left(\frac{7B^2}{4\eta_n} + \frac{\eta_n T \bar{G}_n^2}{2} + \frac{B}{\eta_n} \text{PL}_n^T \right), \quad (7)$$

where we have written $\bar{G}_n \triangleq \sum_{m \in \mathcal{W}_n} w_{n,m} G_m$ and the path-length is defined as

$$\text{PL}_n^T = \sum_{t=2}^T \|\mathbf{U}_{n,t-1} - \mathbf{U}_{n,t}\|. \quad (8)$$

By setting an appropriate learning rate and selecting proper comparator sequences, the regret (7) can be further simplified, as stated in the following corollary.

Corollary 1. By setting $\eta_n = B\sqrt{7}/\bar{G}_n\sqrt{2T}$, the dynamic regret is upper bounded by

$$\begin{aligned} \text{D-Reg}(T) &\leq \sum_{n \in \mathcal{N}} \left(\sqrt{\frac{7}{2}} B \bar{G}_n \sqrt{T} + \sqrt{\frac{2}{7}} \bar{G}_n \text{PL}_n^T \sqrt{T} \right) \\ &= \mathcal{O} \left(\sum_{n \in \mathcal{N}} (1 + \text{PL}_n^T) \sqrt{T} \right). \end{aligned} \quad (9)$$

Furthermore, by letting $\mathbf{U}_{n,t} = \mathbf{U}_n^*$ in (3), the path-length vanishes, i.e., $\text{PL}_n^T = 0$, and the dynamic regret reduces to the static regret, yielding the upper bound

$$\text{S-Reg}(T) \leq \sum_{n \in \mathcal{N}} \left(\sqrt{\frac{7}{2}} B \bar{G}_n \sqrt{T} \right) = \mathcal{O}(N\sqrt{T}). \quad (10)$$

Corollary 1 demonstrates that OGD achieves a dynamic regret that scales with the path-length and thus with the degree of environmental variation. In particular, if the environment is

stationary, the dynamic regret reduces to the static regret (10), which is sublinear in the time horizon T . These results establish upper bounds on the regret achievable by decentralized protocols, in which each agent can only observe local data.

B. Consensus DDAM

In this subsection, we consider a special case of the DDAM problem introduced in the previous section in which all the logical weights in the cost function (2) are equal, i.e., the weight matrix is set to $\mathbf{W} = \mathbb{1}\mathbb{1}^T/N$. In this setting, the cost functions in (2) become identical for all agents $n \in \mathcal{N}$. Therefore, there exists a shared optimal AM mechanism \mathbf{U}^* for all agents, i.e., $\mathbf{U}_n^* = \mathbf{U}^*$.

Under the consensus protocol, all agents asymptotically agree on a common solution \mathbf{X} , i.e., $\mathbf{X}_{n,t} \rightarrow \mathbf{X}$ as $t \rightarrow \infty$. Since this comes with no loss of generality in this setting, we focus here on *consensus distributed OGD* (C-DOGD) [34] to address the DDAM problem in this special case. C-DOGD is specified by an $N \times N$ doubly stochastic matrix \mathbf{A} with entries $[\mathbf{A}]_{n,m} = a_{n,m}$ for all $n \in \mathcal{N}$ and $m \in \mathcal{N}$. In particular, C-DOGD performs local gradient steps followed by consensus averaging as

$$\mathbf{X}_{n,t+1} = \Pi_{\mathcal{X}} \left[\sum_{m \in \mathcal{N}_n} a_{n,m} \mathbf{X}_{m,t} - \eta_n \nabla f_{n,t}(\mathbf{X}_{n,t}) \right], \quad (11)$$

where η_n is the learning rate.

To implement the update (11), each agent n needs to communicate with its neighbors in the set \mathcal{N}_n to exchange the local AM parameters. As a result, all edges in the graph \mathcal{G} are activated, each sustaining a communication load of

$$C_{\max} = 2 \quad (12)$$

AM parameters per iteration.

The static regret properties of C-DOGD follow directly from [34].

Theorem 2. *In the special case $\mathbf{W} = \mathbb{1}\mathbb{1}^T/N$, under Assumptions 1–3, with $\eta_n = 1/2\sqrt{T}$, the C-DOGD protocol obtains the static regret [34, Theorem 1]*

$$\text{S-Reg}(T) \leq N \left(B + \frac{5-\alpha}{1-\alpha} G_{\max}^2 \right) \sqrt{T} = \mathcal{O} \left(N\sqrt{T} \right), \quad (13)$$

where we have defined $G_{\max} = \max_{n \in \mathcal{N}} G_n$ and α is the spectral gap of the doubly stochastic matrix \mathbf{A} .

Although C-DOGD circumvents the need for global loss information, its sublinear static regret guarantee in (13) holds only in the special case where all agents aim to memorize the same information. Furthermore, to the best of our knowledge, the dynamic regret performance of C-DOGD has yet to be investigated.

IV. DISTRIBUTED DYNAMIC ASSOCIATIVE MEMORY VIA TREE-BASED ONLINE GRADIENT DESCENT

In this section, we study the DDAM problem introduced in Sec. II in its full generality by proposing a new protocol, *DDAM via tree-based OGD* (DDAM-TOGD), which will be demonstrated to exhibit guaranteed regret properties.

A. DDAM-TOGD

Recall that in the DDAM problem introduced in Sec. II each agent n aims at memorizing data from a subset \mathcal{W}_n of agents. DDAM-TOGD addresses this problem by enabling inter-agent communication over routing trees connecting each agent n to all relevant agents in $\mathcal{W}_n \setminus \{n\}$ on the physical connectivity graph \mathcal{G} . Based on the delayed information received from the agents in subset $\mathcal{W}_n \setminus \{n\}$, each agent n applies a form of OGD on the cumulative cost in (2).

To elaborate, given the physical communication graph \mathcal{G} and the logical weight matrix \mathbf{W} , DDAM-TOGD first constructs N routing trees $\{\mathcal{T}_n\}_{n \in \mathcal{N}}$. Each tree \mathcal{T}_n is rooted at agent n and contains paths, i.e., sequences of contiguous edges in graph \mathcal{G} , from agent n to all agents in subset \mathcal{W}_n . The construction of the trees is arbitrary, but we will introduce an optimized design based on the regret analysis in Sec. IV-C.

At each time step t , agent n sends its current iterate $\mathbf{X}_{n,t}$ along tree \mathcal{T}_n toward all agents $m \in \mathcal{W}_n \setminus \{n\}$. This information requires $\tilde{\tau}_{n,m}$ time steps to arrive at agent m , where $\tilde{\tau}_{n,m}$ is the number of edges on the path from agent n to agent m . Upon receiving the query at time $t + \tilde{\tau}_{n,m}$, agent m evaluates the gradient $\nabla f_{m,t}(\mathbf{X}_{n,t})$ of the cost corresponding to the data $(\mathbf{k}_{m,t}, \mathbf{v}_{m,t})$, and sends it back along the reverse path. We denote as $\tau_{n,m} = 2\tilde{\tau}_{n,m}$ the total communication delay incurred in the round-trip exchange between agent n and agent m .

Accordingly, the agent n receives the gradient $\nabla f_{m,t}(\mathbf{X}_{n,t})$ at time $t + \tau_{n,m}$. Using the most recent gradient information available from the agents in the subset $m \in \mathcal{W}_n \setminus \{n\}$, at time step $t + 1$, each agent applies the update

$$\mathbf{X}_{n,t+1} = \Pi_{\mathcal{X}} \left[\mathbf{X}_{n,t} - \eta_n \sum_{m \in \mathcal{W}_n} w_{n,m} \mathbf{G}_{m,t-\tau_{n,m}}^n \mathbb{1}_{\{t > \tau_{n,m}\}} \right], \quad (14)$$

where $\mathbf{G}_{m,t-\tau_{n,m}}^n = \nabla f_{m,t-\tau_{n,m}}(\mathbf{X}_{n,t-\tau_{n,m}})$, and η_n is the learning rate. In (14), the gradient corresponding to agent m is multiplied by the weight $w_{n,m}$, reflecting the structure of the cumulative cost function (2). The overall DDAM-TOGD is summarized in Algorithm 1.

For each agent n and each edge $e \in \mathcal{E}$, let $C_{n,m,e} \in \{0, 1\}$ be a binary variable indicating whether the routing tree \mathcal{T}_n includes edge e for delivering a message from the root node n to a target agent m . Specifically, $C_{n,m,e} = 1$ if edge e is used in the path from n to m , and $C_{n,m,e} = 0$ otherwise. The overall maximum per-link capacity required by DDAM-TOGD for a given choice $\mathcal{T} = \{\mathcal{T}_n\}$ of trees is thus given by

$$C_{\max}^{\mathcal{T}} = 2 \max_{e \in \mathcal{E}} \sum_{n \in \mathcal{N}} \sum_{m \in \mathcal{W}_n} C_{n,m,e}. \quad (15)$$

Note that this is generally larger than the per-link capacity (12) required by C-DOGD.

B. Regret Analysis

The regret of the proposed DDAM-TOGD algorithm is characterized in the following theorem.

Algorithm 1 DDAM-TOGD (at agent n)

Input: Learning rate sequences $\{\eta_{n,t}\}_{t \geq 1}$, logical weight $\{w_{n,m}\}_{m \in \mathcal{W}_n}$, and tree \mathcal{T}_n

- 1: **Initialize** AM parameters $\{\mathbf{X}_{n,1}\}_{n \in \mathcal{N}}$
- 2: **for** $t = 1, 2, \dots$ **do**
- 3: *# Receive memory parameters and send losses*
- 4: Receive $\mathbf{X}_{m,t-\tilde{\tau}_{m,n}}$ from agent m
- 5: Send $\nabla f_{n,t-\tilde{\tau}_{m,n}}(\mathbf{X}_{m,t-\tilde{\tau}_{m,n}})$ to agent m
- 6: *# Send memory parameter and receive losses*
- 7: Broadcast $\mathbf{X}_{n,t}$ to all agents $m \in \mathcal{W}_n \setminus \{n\}$
- 8: Receive $\nabla f_{m,t-\tau_{n,m}}(\mathbf{X}_{n,t-\tau_{n,m}})$ from all agents $m \in \mathcal{W}_n \setminus \{n\}$
- 9: *# Online Gradient Descent*
- 10: Update local memory parameter using (14)
- 11: **end for**

Theorem 3. Under Assumptions 1–3, the dynamic regret of the proposed DDAM-TOGD protocol satisfies the upper bound

$$\begin{aligned} \text{D-Reg}(T) \leq \sum_{n \in \mathcal{N}} \left(Q_n \eta_n (T + \Delta \tau_n) + J_n \eta_n + \frac{7B^2}{4\eta_n} \right. \\ \left. + \left(\frac{B}{\eta_n} + H_n \right) \text{PL}_n^{T+\tau_{n,\max}} + C_n \right), \end{aligned} \quad (16)$$

where

$$Q_n = \frac{1}{2} K_n \left(\sum_{m \in \mathcal{W}_n} G_m \right) + |\mathcal{W}_n| K_n^2 \tau_{n,\text{sum}}, \quad (17)$$

$$J_n = |\mathcal{W}_n|^2 K_n^2 \tau_{n,\max}^2, \quad (18)$$

$$H_n = K_n \tau_{n,\text{sum}}, \quad (19)$$

$$C_n = K_n \Delta \tau_n |\mathcal{W}_n| B, \quad (20)$$

with

$$K_n = \max_m w_{n,m} G_m, \quad (21)$$

$$\tau_{n,\min} = \min_m \tau_{n,m}, \quad (22)$$

$$\tau_{n,\max} = \max_m \tau_{n,m}, \quad (23)$$

$$\Delta \tau_n = \tau_{n,\max} - \tau_{n,\min}, \quad (24)$$

$$\tau_{n,\text{sum}} = \sum_{m \in \mathcal{W}_n} \tau_{n,m}. \quad (25)$$

The proof of Theorem 3 is discussed in Sec. V. Based on Theorem 3, by specifying the learning rate, the static and dynamic regrets can be specialized as stated in the following corollary.

Corollary 2. By setting $\eta_n = \sqrt{7B^2/4(Q_n(T + \Delta \tau_n) + J_n)}$, the dynamic regret of proposed DDAM-TOGD is upper bounded by

$$\begin{aligned} \text{D-Reg}(T) \\ \leq \sum_{n \in \mathcal{N}} \left(\sqrt{7} B \sqrt{Q_n(T + \Delta \tau_n) + J_n} \right. \\ \left. + \left(H_n + \frac{2}{\sqrt{7}} \sqrt{Q_n(T + \Delta \tau_n) + J_n} \right) \text{PL}_n^{T+\tau_{n,\max}} \right) \end{aligned}$$

$$= \mathcal{O} \left(\sum_{n \in \mathcal{N}} \left((1 + \text{PL}_n^{T+\tau_{n,\max}}) \sqrt{(1 + \tau_{n,\text{sum}})(T + \Delta \tau_n)} \right) \right). \quad (26)$$

Furthermore, by letting $\mathbf{U}_{n,t} = \mathbf{U}_n^*$ in (3), the path-length vanishes, i.e., $\text{PL}_n^T = 0$, and the dynamic regret reduces to the static regret, yielding the upper bound

$$\begin{aligned} \text{S-Reg}(T) &\leq \sum_{n \in \mathcal{N}} \sqrt{7} B \sqrt{Q_n(T + \Delta \tau_n) + J_n} \\ &= \mathcal{O} \left(\sum_{n \in \mathcal{N}} \sqrt{(1 + \tau_{n,\text{sum}})(T + \Delta \tau_n)} \right). \end{aligned} \quad (27)$$

From Corollary 2, DDAM-TOGD achieves the dynamic regret bound in (26). Compared with the dynamic regret of the idealized OGD in (9), where the path-length is scaled by the factor \sqrt{T} , the path-length in DDAM-TOGD is scaled by the term $\sqrt{(1 + \tau_{n,\text{sum}})(T + \Delta \tau_n)}$, making the regret explicitly dependent on the communication delay. In fact, the quantity $\tau_{n,\text{sum}}$ in (25) is the cumulative delay from agent n to all agents of interest in \mathcal{W}_n ; while the quantity $\Delta \tau_n$ in (24) is the difference between the maximum and minimum delays from agent n .

This dependence on the delay reflects the fact that information exchange in the distributed network slows down the learning progress of the AM process. When the time horizon T is much larger than the sum-delay $\tau_{n,\text{sum}}$, the coefficient $\sqrt{(1 + \tau_{n,\text{sum}})(T + \Delta \tau_n)}$ remains sublinear in T , and thus DDAM-TOGD achieves the same sublinear time dependency as the idealized OGD. The same conclusions hold for the static regret (27).

C. Design of Communication Trees

The proposed DDAM-TOGD protocol applies to any choice of the routing trees \mathcal{T}_n connecting each agent n to all the agents $m \in \mathcal{W}_n$, whose data must be memorized by agent n . However, the regret bounds in (26) and (27) provide useful insights into the design of the routing trees $\{\mathcal{T}_n\}_{n \in \mathcal{N}}$. In particular, the upper bound highlights the influence of the term $(1 + \tau_{n,\text{sum}})(T + \Delta \tau_n)$ on each agent's performance. As discussed in the previous subsection, when the memorization horizon T is large enough, the dominant component of the regret bound is the cumulative delay term $\tau_{n,\text{sum}}$. Based on these insights, we propose to design the trees \mathcal{T}_n with the aim of minimizing the sum-delay $\tau_{n,\text{sum}}$. The proposed combinatorial optimization procedure is detailed in Appendix E, and we refer to the resulting scheme as DDAM-TOGD*.

V. THEORETICAL ANALYSIS

In this section, we outline the proof of Theorem 3, with additional details provided in the Appendix. The proof proceeds by first decomposing the dynamic regret (5) to isolate the impact of communication delays and then bounding each constituent term separately.

A. Regret Decomposition

The network dynamic regret (5) can be expressed as the sum of the local dynamic regrets of all agents as

$$\begin{aligned} \text{D-Reg}(T) &= \sum_{n \in \mathcal{N}} \underbrace{\left(\mathcal{L}_n^T(\mathbf{X}_n^T) - \mathcal{L}_n^T(\mathbf{U}_n^T) \right)}_{\text{D-Reg}_n(T)} \\ &= \sum_{n \in \mathcal{N}} \text{D-Reg}_n(T). \end{aligned} \quad (28)$$

We next derive a bound for the dynamic regret of each agent n , i.e., $\text{D-Reg}_n(T)$. Summing these bounds over all agents yields an overall network-level guarantee. To start, the local dynamic regret of agent n can be upper bounded in a convenient way that isolates the contributions of communication delays

$$\begin{aligned} \text{D-Reg}_n(T) &= \mathcal{L}_n^T(\mathbf{X}_n^T) - \mathcal{L}_n^T(\mathbf{U}_n^T) \\ &\stackrel{(a)}{\leq} \sum_{t=1}^T \sum_{m \in \mathcal{W}_n} w_{n,m} \langle \mathbf{G}_{m,t}^n, \mathbf{X}_{n,t} - \mathbf{U}_{n,t} \rangle \\ &\stackrel{(b)}{=} \sum_{m \in \mathcal{W}_n} \sum_{t=\tau_{n,m}+1}^{T+\tau_{n,m}} w_{n,m} \langle \mathbf{G}_{m,t-\tau_{n,m}}^n, \mathbf{X}_{n,t-\tau_{n,m}} - \mathbf{U}_{n,t-\tau_{n,m}} \rangle \\ &= \underbrace{\sum_{t=\tau_{n,\min}+1}^{T+\tau_{n,\max}} \sum_{m \in \mathcal{W}_n} w_{n,m} \langle \mathbf{G}_{m,t-\tau_{n,m}}^n \mathbb{1}_{\{t > \tau_{n,m}\}}, \mathbf{X}_{n,t} - \mathbf{U}_{n,t} \rangle}_{\text{Reg}^*} \\ &\quad + \underbrace{\sum_{m \in \mathcal{W}_n} \sum_{t=\tau_{n,m}+1}^{T+\tau_{n,m}} w_{n,m} \langle \mathbf{G}_{m,t-\tau_{n,m}}^n, \mathbf{X}_{n,t-\tau_{n,m}} - \mathbf{X}_{n,t} \rangle}_{\text{Drift}_{\mathbf{X}}} \\ &\quad + \underbrace{\sum_{m \in \mathcal{W}_n} \sum_{t=\tau_{n,m}+1}^{T+\tau_{n,m}} w_{n,m} \langle \mathbf{G}_{m,t-\tau_{n,m}}^n, \mathbf{U}_{n,t} - \mathbf{U}_{n,t-\tau_{n,m}} \rangle}_{\text{Drift}_{\mathbf{U}}} \\ &\quad + \underbrace{\sum_{m \in \mathcal{W}_n} \sum_{t=T+\tau_{n,m}+1}^{T+\tau_{n,\max}} w_{n,m} \langle \mathbf{G}_{m,t-\tau_{n,m}}^n, \mathbf{U}_{n,t} - \mathbf{X}_{n,t} \rangle}_{\text{Tail}}, \end{aligned} \quad (29)$$

where (a) holds by the convexity of the local loss functions [8, Lemma 2.5], and (b) holds by changing the order of summation and adjusting the start and end indices. In the decomposition (29), the term Reg^* retains the characteristic form of conventional regret analyses [7], while the remaining terms, namely $\text{Drift}_{\mathbf{X}}$, $\text{Drift}_{\mathbf{U}}$, and Tail , are consequences of the presence of communication delays. Specifically, the terms $\text{Drift}_{\mathbf{X}}$ and $\text{Drift}_{\mathbf{U}}$ quantify the drift caused by the mismatch between stale and current iterates in the decision and comparator sequences, respectively; while the term Tail accounts for gradient information that arrives only after the horizon T and hence cannot be incorporated into the updates.

B. Bounding Individual Terms

We now analyze each term separately. Combining the bounds below immediately yields Theorem 3.

1) *Bounding Reg^** : Following [7, Lemma 2.12], we first establish the following key lemma.

Lemma 1. *Under Assumption 3, the DDAM-TOGD update rule in (14) satisfies the following inequality*

$$\begin{aligned} &\sum_{m \in \mathcal{W}_n} \left\langle w_{n,m} \mathbf{G}_{m,t-\tau_{n,m}}^n \mathbb{1}_{\{t > \tau_{n,m}\}}, \mathbf{X}_{n,t} - \mathbf{U}_{n,t} \right\rangle \\ &\leq \frac{\|\mathbf{X}_{n,t} - \mathbf{U}_{n,t}\|^2 - \|\mathbf{X}_{n,t+1} - \mathbf{U}_{n,t}\|^2}{2\eta_n} \\ &\quad + K_n \left(\sum_{m \in \mathcal{W}_n} G_m \right) \frac{\eta_n}{2}, \end{aligned} \quad (30)$$

where K_n is defined in (21).

Proof: See Appendix A. ■

Summing (30) over index t from τ_{\min} to $T + \tau_{\max}$ gives the upper bound

$$\begin{aligned} \text{Reg}^* &= \sum_{t=\tau_{n,\min}+1}^{T+\tau_{n,\max}} \sum_{m \in \mathcal{W}_n} w_{n,m} \langle \mathbf{G}_{m,t-\tau_{n,m}}^n \mathbb{1}_{\{t > \tau_{n,m}\}}, \mathbf{X}_{n,t} - \mathbf{U}_{n,t} \rangle \\ &\leq \frac{1}{2} K_n \left(\sum_{m \in \mathcal{W}_n} G_m \right) \eta_n (T + \Delta\tau_n) \\ &\quad + \sum_{t=\tau_{n,\min}+1}^{T+\tau_{n,\max}} \frac{\|\mathbf{X}_{n,t} - \mathbf{U}_{n,t}\|^2 - \|\mathbf{X}_{n,t+1} - \mathbf{U}_{n,t}\|^2}{2\eta_n}. \end{aligned} \quad (31)$$

Theorem 4. *Under Assumption 2, the telescoping term in (31) can be bounded as*

$$\begin{aligned} &\sum_{t=\tau_{n,\min}+1}^{T+\tau_{n,\max}} \frac{\|\mathbf{X}_{n,t} - \mathbf{U}_{n,t}\|^2 - \|\mathbf{X}_{n,t+1} - \mathbf{U}_{n,t}\|^2}{2\eta_n} \\ &\leq \frac{B}{\eta_n} \text{PL}_n^{T+\tau_{n,\max}} + \frac{7B^2}{4\eta_n}. \end{aligned} \quad (32)$$

Proof: See Appendix B. ■

Plugging (32) into (31), Reg^* is bounded as

$$\begin{aligned} \text{Reg}^* &\leq \frac{1}{2} K_n \left(\sum_{m \in \mathcal{W}_n} G_m \right) \eta_n (T + \Delta\tau_n) \\ &\quad + \frac{B}{\eta_n} \text{PL}_n^{T+\tau_{n,\max}} + \frac{7B^2}{4\eta_n}. \end{aligned} \quad (33)$$

2) *Bounding $\text{Drift}_{\mathbf{X}}$* : By applying the Cauchy-Schwarz inequality together with Assumption 3, $\text{Drift}_{\mathbf{X}}$ is bounded as

$$\begin{aligned} \text{Drift}_{\mathbf{X}} &= \sum_{m \in \mathcal{W}_n} \sum_{t=\tau_{n,m}+1}^{T+\tau_{n,m}} w_{n,m} \langle \mathbf{G}_{m,t-\tau_{n,m}}^n, \mathbf{X}_{n,t-\tau_{n,m}} - \mathbf{X}_{n,t} \rangle \\ &\leq \sum_{m \in \mathcal{W}_n} \sum_{t=\tau_{n,m}+1}^{T+\tau_{n,m}} w_{n,m} G_m \|\mathbf{X}_{n,t} - \mathbf{X}_{n,t-\tau_{n,m}}\| \\ &\leq \sum_{m \in \mathcal{W}_n} \sum_{t=\tau_{n,m}+1}^{T+\tau_{n,m}} K_n \|\mathbf{X}_{n,t} - \mathbf{X}_{n,t-\tau_{n,m}}\|. \end{aligned} \quad (34)$$

Thus, the bound of $\text{Drift}_{\mathbf{X}}$ depends on the term $\|\mathbf{X}_{n,t} - \mathbf{X}_{n,t-\tau_{n,m}}\|$, which measures the difference between the variables with and without delay. Unrolling the difference

$\mathbf{X}_{n,t} - \mathbf{X}_{n,t-\tau_{n,m}}$ for $t > \tau_{n,m}$ and from the update rule (14), we obtain the inequality

$$\begin{aligned} \|\mathbf{X}_{n,t} - \mathbf{X}_{n,t-\tau_{n,m}}\| &= \left\| \sum_{j=1}^{\tau_{n,m}} (\mathbf{X}_{n,t-j+1} - \mathbf{X}_{n,t-j}) \right\| \\ &\leq \eta_m K_n \sum_{s \in \mathcal{W}_n} \min\{\tau_{n,m}, t - \tau_{n,s} - 1\}. \end{aligned} \quad (35)$$

Substituting (35) into (34) and after some algebraic manipulation, $\text{Drift}_{\mathbf{X}}$ can be bounded by

$$\begin{aligned} \text{Drift}_{\mathbf{X}} &\leq |\mathcal{W}_n|^2 K_n^2 \tau_{n,\max}^2 \eta_n \\ &\quad + |\mathcal{W}_n| K_n^2 \tau_{n,\text{sum}} \eta_n (T + \Delta \tau_n). \end{aligned} \quad (36)$$

The detailed derivations of (35) and (36) can be found in Appendix C.

3) *Bounding $\text{Drift}_{\mathbf{U}}$* : By applying the Cauchy-Schwarz inequality together with Assumption 3, we obtain

$$\begin{aligned} \text{Drift}_{\mathbf{U}} &= \sum_{m \in \mathcal{W}_n} \sum_{t=\tau_{n,m}+1}^{T+\tau_{n,m}} w_{n,m} \langle \mathbf{G}_{m,t-\tau_{n,m}}^n, \mathbf{U}_{n,t} - \mathbf{U}_{n,t-\tau_{n,m}} \rangle \\ &\leq \sum_{m \in \mathcal{W}_n} \sum_{t=\tau_{n,m}+1}^{T+\tau_{n,m}} w_{n,m} G_m \|\mathbf{U}_{n,t} - \mathbf{U}_{n,t-\tau_{n,m}}\| \\ &\leq K_n \sum_{m \in \mathcal{W}_n} \sum_{t=\tau_{n,m}+1}^{T+\tau_{n,m}} \|\mathbf{U}_{n,t} - \mathbf{U}_{n,t-\tau_{n,m}}\|. \end{aligned} \quad (37)$$

The expression (37) reveals that the term $\text{Drift}_{\mathbf{U}}$ arises to the discrepancy between the comparator sequences with and without delay.

Lemma 2. *The drift of the comparator caused by delay can be bounded as*

$$\sum_{t=\tau_{n,m}+1}^{T+\tau_{n,m}} \|\mathbf{U}_{n,t} - \mathbf{U}_{n,t-\tau_{n,m}}\| \leq \tau_{n,m} \text{PL}_n^{T+\tau_{n,m}}. \quad (38)$$

Proof: See Appendix D.

With Lemma 2, $\text{Drift}_{\mathbf{U}}$ can be bounded as

$$\begin{aligned} \text{Drift}_{\mathbf{U}} &\leq K_n \sum_{m \in \mathcal{W}_n} \sum_{t=\tau_{n,m}+1}^{T+\tau_{n,m}} \|\mathbf{U}_{n,t} - \mathbf{U}_{n,t-\tau_{n,m}}\| \\ &\leq K_n \sum_{m \in \mathcal{W}_n} \tau_{n,m} \sum_{t=2}^{T+\tau_{n,m}} \text{PL}_n^{T+\tau_{n,m}} \\ &\stackrel{(a)}{\leq} K_n \tau_{n,\text{sum}} \text{PL}_n^{T+\tau_{n,\max}}, \end{aligned} \quad (39)$$

where (a) follows from the inequality $\text{PL}_n^{T+\tau_{n,m}} \leq \text{PL}_n^{T+\tau_{n,\max}}$ for all $m \in \mathcal{W}_n$.

4) *Bounding Tail*: By applying the Cauchy-Schwarz inequality together with Assumptions 2 and 3, we obtain

$$\begin{aligned} \text{Tail} &= \sum_{m \in \mathcal{W}_n} \sum_{t=T+\tau_{n,m}+1}^{T+\tau_{n,\max}} w_{n,m} \langle \mathbf{G}_{m,t-\tau_{n,m}}^n, \mathbf{U}_{n,t} - \mathbf{X}_{n,t} \rangle \\ &\leq \sum_{m \in \mathcal{W}_n} \sum_{t=T+\tau_{n,m}+1}^{T+\tau_{n,\max}} w_{n,m} G_m \|\mathbf{U}_{n,t} - \mathbf{X}_{n,t}\| \\ &\leq K_n \Delta \tau_n |\mathcal{W}_n| B, \end{aligned} \quad (40)$$

concluding the proof.

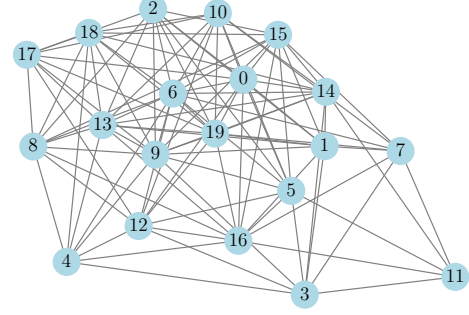


Fig. 2. Physical topology considered in the experiments.

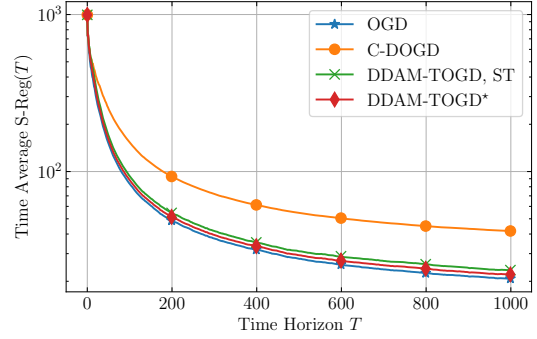


Fig. 3. Regret versus time horizon T ($\rho = 0.75$, $y_0 = 2$, and $y_1 = 10$).

VI. EXPERIMENTS

In this section, we empirically evaluate the performance of the proposed DDAM-TOGD using a synthetic dataset and a real wireless traffic dataset [14].

A. Synthetic Dataset

We consider memorization under the DeltaNet model [21], where memory retrieval is linear and the loss function for agent n at time t is given by the third entry in Table I. The key vectors $\mathbf{k}_{n,t}$ are generated independently for each agent n and time t , by drawing each entry from a uniform distribution over the interval $[-1, 1]$. The corresponding value vectors $\mathbf{v}_{n,t}$ are generated as

$$\mathbf{v}_{n,t} = ((1 - \rho)\mathbf{M}_n^* + \rho\mathbf{M}_{\text{com}}^*) \mathbf{k}_{n,t} + \mathbf{n}_{n,t}, \quad (41)$$

where $\mathbf{n}_{n,t} \sim \mathcal{N}(0, \sigma_n^2)$ denotes additive Gaussian noise, with $\sigma_n^2 = 1$. The data-generation model (41) indicates that, apart from the presence of noise, the ground-truth optimal linear mechanism for agent n is given by $(1 - \rho)\mathbf{M}_n^* + \rho\mathbf{M}_{\text{com}}^*$, combining a personalized component \mathbf{M}_n^* and a common component $\mathbf{M}_{\text{com}}^*$ shared across all agents. The correlation parameter $\rho \in [0, 1]$ controls the trade-off between personalized and common memory contributions. Matrix $\mathbf{M}_{\text{com}}^*$ is generated by sampling each entry independently from a chi-squared distribution with 2 degrees of freedom, while the matrices \mathbf{M}_n^* are generated independently with Gaussian entries $\mathbf{M}_n^* \sim \mathcal{N}(\mu_n, \sigma_n^2)$, where the mean μ_n and variance σ_n^2 are independently and uniformly sampled from the intervals $[-5, 5]$ and $[0, 50]$, respectively.

The logical weight matrix \mathbf{W} is constructed such that each n -th row is sampled independently from a Dirichlet

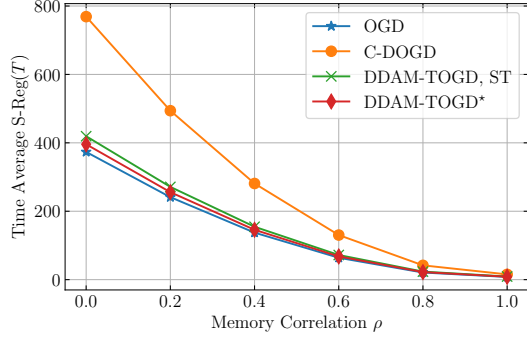


Fig. 4. Regret at $T = 2500$ versus memory correlation parameter ρ ($y_0 = 6$, and $y_1 = 10$).

distribution. Specifically, the n -th row is determined as the random vector

$$\mathbf{W}[n, :] \sim \text{Dirichlet}(\underbrace{y_0, \dots, y_0}_{1:n-1}, y_1, \underbrace{y_0, \dots, y_0}_{n+1:N}), \quad (42)$$

for some $y_1 \geq y_0 \geq 0$. This way, the weight in (42) assigned to the local data at agent n is, on average, more relevant than the data from other agents by a factor y_1/y_0 . The number of agents is set to $N = 20$, and the connecting graph is shown in Fig. 2.

To ensure a fair comparison, given a time horizon T for OGD and C-DOGD, we set the time horizon for DDAM-TOGD as T/C_{\max}^T , where the maximum per-link capacity C_{\max}^T for a given choice of trees \mathcal{T} is defined in (15). This accounts for the fact that a single iteration may take up to $1/C_{\max}^T$ more time in DDAM-TOGD as compared to C-DOGD, since the link with the largest load must communicate C_{\max}^T messages per iteration. For DDAM-TOGD, we consider a baseline version using Steiner trees, referred to as “DAM-TOGD (ST)”, with DDAM-TOGD* defined as in Section IV-C. Recall that Steiner trees optimize the total edge weight, while the design introduced in Section IV-C minimizes the total path-length. The time average static regret of the network at time horizon T is $\text{S-Reg}(T)/T$.

Convergence: In Fig. 3, we study the evolution of the time average static regret (4) over time for OGD, C-DOGD, and the proposed DDAM-TOGD. As evidenced by the consistent decline in regret with increasing time horizon T seen in Fig. 3, both OGD and the proposed DDAM-TOGD exhibit a clear sublinear regret trend, conforming to Theorem 3 and Corollary 2. In contrast, the regret of C-DOGD initially decreases but quickly plateaus, demonstrating a regret behavior that fails to improve with time. This is because C-DOGD forces the agents to use the same memory mechanism as time t increases, while the model (41) implies that different memorization mechanisms are preferred at different agents.

Impact of Memory Correlation: Fig. 4 shows the effect of the memory correlation parameter ρ in (41) on the regret. For large ρ , memory heterogeneity is minimal and all methods perform similarly. As ρ decreases, personalization increases, consensus becomes restrictive, and C-DOGD suffers a rapidly growing regret. In contrast, DDAM-TOGD mitigates hetero-

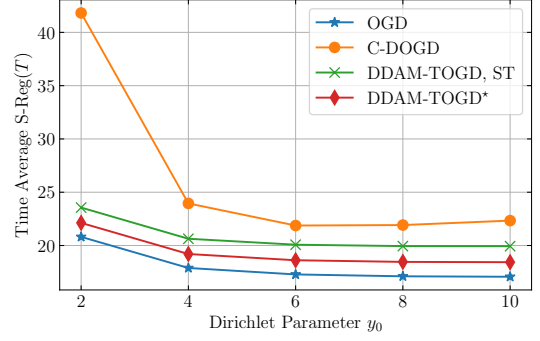


Fig. 5. Regret at $T = 2500$ versus Dirichlet parameter y_0 ($\rho = 0.75$, and $y_1 = 10$).

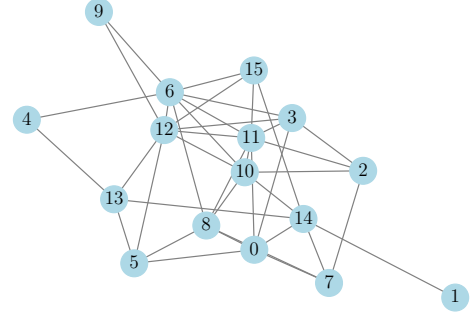


Fig. 6. Physical topology considered in the experiments with the wireless traffic dataset.

geneity and maintains low regret, demonstrating robustness to personalization.

Impact of the Logical Weight Matrix: In Fig. 5, we report the effect of the logical weight matrix in (42) by varying the Dirichlet parameter y_0 (with $y_1 = 10$), which controls how each agent’s memory incorporates data from others. When the parameter y_0 is small, the weight matrix \mathbf{W} becomes highly imbalanced, emphasizing personalized weights. In this regime, achieving consensus does not result in the optimal solution and C-DOGD incurs a large regret. In contrast, the results show that OGD and the proposed DDAM-TOGD methods are largely unaffected by variations in parameter y_0 , demonstrating their robustness to changes in the network logical weight structure.

B. Wireless Traffic Dataset

In this experiment, we evaluate wireless traffic usage memorization using real traffic data from an enterprise network [14]. The dataset consists of measurements collected from 470 access points (APs). In our experiment, we focus on $N = 16$ APs randomly selected from the “High” group [14], which consists of 79 APs with the highest mean traffic usage. To reduce the dynamic range of inputs, raw traffic measurements are preprocessed using a logarithmic transformation. In this experiment, the connection graph is randomly generated, where each pair of nodes is connected with probability 0.25. The resulting graph is illustrated in Fig. 6.

In this dataset, the transmitted traffic volume was recorded every 10 minutes between December 20, 2018 and February 8, 2019 [14]. Thus, each hour consists of six consecutive samples

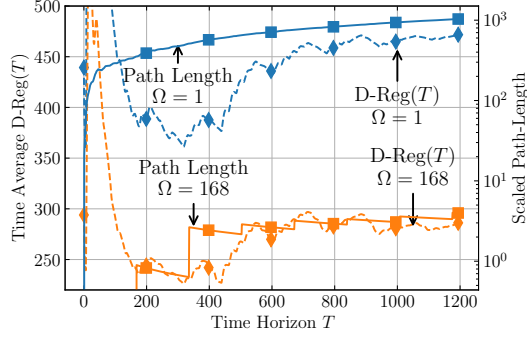


Fig. 7. Regret of proposed DDAM-TOGD* and scaled path-length versus time horizon T with different Ω ($y_0 = 10$, and $y_1 = 100$).

for every AP. For each AP n and time step t , we form a key-value pair $(\mathbf{k}_{n,t}, \mathbf{v}_{n,t})$, where the value $\mathbf{v}_{n,t} \in \mathbb{R}^{d_v}$ aggregates the six ($d_v = 6$) 10-minute traffic measurements of AP n within the hour associated with time step t . The corresponding key is constructed as $\mathbf{k}_{n,t} = [\mathbf{k}_{\text{AP},n}; \mathbf{k}_{\text{time},t}] \in \mathbb{R}^{d_k}$, where $\mathbf{k}_{\text{AP},n} = \Phi_{\text{AP}}(n) \in \mathbb{R}^{d_{\text{AP}}}$ specifies the identity of the n -th AP, and $\mathbf{k}_{\text{time},t} = \Phi_{\text{time}}(t \bmod 24) \in \mathbb{R}^{d_{\text{time}}}$ encodes the hour-of-day associated with time step t . The temporal embedding function Φ_{time} uses Transformer-style sinusoidal (cos/sin) embeddings [3], whereas the AP embedding function Φ_{AP} combines a one-hot representation of the AP index with a Transformer-style sinusoidal embedding. In our experiments, we set $d_{\text{AP}} = 24$, and $d_{\text{time}} = 10$.

To evaluate the dynamic regret, we use as a reference a comparator $\mathbf{U}_{n,t}$ that is optimized in hindsight separately, for each time window $\Theta_k \triangleq \{(k-1)\Omega + 1, \dots, k\Omega\}$ with $k = 1, 2, \dots$, of duration Ω time intervals, i.e., $\Omega \times 10$ minutes. Accordingly, we select the comparator $\mathbf{U}_{n,t}$, for all $t \in \Theta_k$, as

$$\mathbf{U}_{n,t} \in \arg \min_{\mathbf{U} \in \mathcal{X}} \sum_{s \in \Theta_k} \sum_{m \in \mathcal{W}_n} w_{n,m} f_{m,s}(\mathbf{U}), \quad (43)$$

If $\Omega = 1$, the comparator (43) can change at every time step, while if Ω equals the time horizon T , the comparator (43) reduces to the hindsight-optimal static solution in (3), yielding the static-regret criterion.

The time-horizon scaling method and logical weights are set in the same way as in the synthetic-dataset case described in the previous subsection. The time average dynamic regret of network at time horizon T is evaluated as the ratio $\text{D-Reg}(T)/T$.

Validation of the relation between dynamic regret and path-length: We plot the dynamic regret for the proposed DDAM-TOGD* with different time window size Ω in Fig. 7. To validate the bounds (27), we also show the quantity $(1 + \text{PL}_n^T)/\sqrt{T}$, which describes the scaling of the bounds on the time-averaged dynamic regret. When $\Omega = 1$, the comparator may change at every time step, causing the path-length to increase rapidly. In contrast, when $\Omega = 168$, the comparator changes every week (since $\Omega = 7 \times 24$), and the path-length grows much more slowly. Validating the theoretical bounds, in the case $\Omega = 1$, the dynamic regret also exhibits a fast-increasing trend, whereas for $\Omega = 168$ it grows significantly

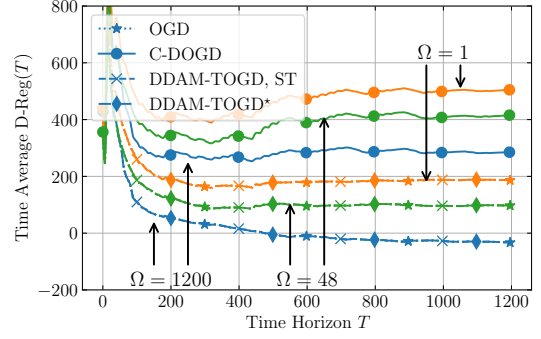


Fig. 8. Regret versus time horizon T ($y_0 = 0.1$, and $y_1 = 100$).

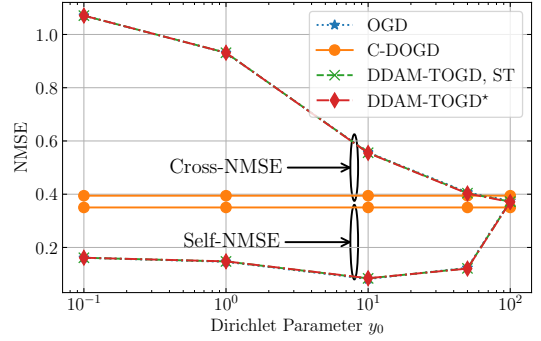


Fig. 9. NMSE versus Dirichlet parameter y_0 ($y_1 = 100$).

more slowly. Overall, the dynamic regret closely follows the evolution of the scaled path-length.

Convergence: In Fig. 8, we study the evolution of the dynamic regret (5) over time for OGD, C-DOGD, and the proposed DDAM-TOGD with different choices of the time window size Ω of the comparators (43). The proposed DDAM-TOGD is seen to approach the ideal centralized solution set by OGD. This shows that in this setting communication delays have a minor impact on performance due to the near-periodicity of the data. In contrast, for C-DOGD, the dynamic regret is much larger than for OGD, indicating the need for specializing the AM mechanisms at the agents. Note also that the static regret, obtained with $\Omega = T = 1200$, can become negative, showing that the hindsight-best solution is not necessarily optimal in a non-stationary environment.

Normalized Mean Squared Error (NMSE) Performance: In addition to the regret performance shown so far, in Fig. 9 we investigate the NMSE performance of memory retrieval. Specifically, we evaluate self-NMSE and cross-NMSE, measuring the error in retrieving one's own value and the ability to recall other APs' traffic usage, respectively, defined as

$$\text{Self-NMSE} = \frac{\sum_t \sum_{n \in \mathcal{N}} \|\mathbf{X}_n \mathbf{k}_{n,t} - \mathbf{v}_{n,t}\|^2}{\sum_t \sum_{n \in \mathcal{N}} \|\mathbf{v}_{n,t}\|^2},$$

$$\text{Cross-NMSE} = \frac{\sum_t \sum_{n \in \mathcal{N}} \sum_{m \in \mathcal{W}_n \setminus \{n\}} \|\mathbf{X}_n \mathbf{k}_{m,t} - \mathbf{v}_{m,t}\|^2}{\sum_t \sum_{n \in \mathcal{N}} \sum_{m \in \mathcal{W}_n \setminus \{n\}} \|\mathbf{v}_{m,t}\|^2}.$$

In Fig. 9, as y_0 increases, each agent places less weight on its own data and more weight on other APs, which enhances its ability to memorize the traffic usage of other APs leading to a decreasing trend in cross-NMSE. Furthermore,

as y_0 increases, the self-NMSE first decreases slightly and then rises sharply. This observation suggests that selectively incorporating information from others can be beneficial, but excessive attention to other agents' data is detrimental.

VII. CONCLUSION

This paper introduced the concept of DDAM and proposed DDAM-TOGD, a tree-based distributed online gradient optimization method that enables agents to build and update AMs under time-varying data streams. We established sublinear static regret and path-length dependent dynamic regret, revealing how communication delay and routing topology affect regret performance. Based on these insights from the theoretical analysis, we proposed a combinatorial optimization based routing-tree design method. Experiments on synthetic datasets and real wireless traffic usage memorization have verified the theory: DDAM-TOGD adapts to changing associations, and achieves lower regret than existing solutions.

Future work includes investigating time-varying connectivity, exploring non-linear associative memory mechanisms, and studying parameter-free online learning algorithms [35].

APPENDIX A PROOF OF LEMMA 1

We first present the following inequality

$$\begin{aligned}
& \frac{1}{2} \|\mathbf{X}_{n,t+1} - \mathbf{U}_{n,t}\|^2 - \frac{1}{2} \|\mathbf{X}_{n,t} - \mathbf{U}_{n,t}\|^2 \\
&= \frac{1}{2} \left\| \Pi_{\mathcal{X}} \left[\mathbf{X}_{n,t} - \eta_n \sum_{m \in \mathcal{W}_n} w_{n,m} \mathbf{G}_{m,t-\tau_{n,m}}^n \mathbb{1}_{\{t > \tau_{n,m}\}} \right] - \mathbf{U}_{n,t} \right\|^2 \\
&\quad - \frac{1}{2} \|\mathbf{X}_{n,t} - \mathbf{U}_{n,t}\|^2 \\
&\stackrel{(a)}{\leq} \frac{1}{2} \left\| \mathbf{X}_{n,t} - \eta_n \sum_{m \in \mathcal{W}_n} w_{n,m} \mathbf{G}_{m,t-\tau_{n,m}}^n \mathbb{1}_{\{t > \tau_{n,m}\}} - \mathbf{U}_{n,t} \right\|^2 \\
&\quad - \frac{1}{2} \|\mathbf{X}_{n,t} - \mathbf{U}_{n,t}\|^2 \\
&= \frac{\eta_n^2}{2} \left\| \sum_{m \in \mathcal{W}_n} w_{n,m} \mathbf{G}_{m,t-\tau_{n,m}}^n \mathbb{1}_{\{t > \tau_{n,m}\}} \right\|^2 \\
&\quad - \eta_n \sum_{m \in \mathcal{W}_n} \left\langle w_{n,m} \mathbf{G}_{m,t-\tau_{n,m}}^n \mathbb{1}_{\{t > \tau_{n,m}\}}, \mathbf{X}_{n,t} - \mathbf{U}_{n,t} \right\rangle, \tag{A-1}
\end{aligned}$$

where (a) holds since $\|\Pi_{\mathcal{X}}[\mathbf{X}] - \mathbf{Y}\|^2 \leq \|\mathbf{X} - \mathbf{Y}\|^2$ for $\mathbf{Y} \in \mathcal{X}$ [7, Proposition 2.11].

Dividing both sides by η_n and rearranging the terms, we obtain

$$\begin{aligned}
& \sum_{m \in \mathcal{W}_n} \left\langle w_{n,m} \mathbf{G}_{m,t-\tau_{n,m}}^n \mathbb{1}_{\{t > \tau_{n,m}\}}, \mathbf{X}_{n,t-\tau_{n,m}} - \mathbf{U}_{n,t} \right\rangle \\
&\leq \frac{\eta_n}{2} \left\| \sum_{m \in \mathcal{W}_n} w_{n,m} \mathbf{G}_{m,t-\tau_{n,m}}^n \mathbb{1}_{\{t > \tau_{n,m}\}} \right\|^2 \\
&\quad + \frac{\|\mathbf{X}_{n,t} - \mathbf{U}_{n,t}\|^2 - \|\mathbf{X}_{n,t+1} - \mathbf{U}_{n,t}\|^2}{2\eta_n}
\end{aligned}$$

$$\begin{aligned}
&\stackrel{(a)}{\leq} \frac{\eta_n}{2} \sum_{m \in \mathcal{W}_n} w_{n,m} \left\| \mathbf{G}_{m,t-\tau_{n,m}}^n \right\|^2 \\
&\quad + \frac{\|\mathbf{X}_{n,t} - \mathbf{U}_{n,t}\|^2 - \|\mathbf{X}_{n,t+1} - \mathbf{U}_{n,t}\|^2}{2\eta_n} \\
&\stackrel{(b)}{\leq} \left(\sum_{m \in \mathcal{W}_n} w_{n,m} G_m^2 \right) \frac{\eta_n}{2} \\
&\quad + \frac{\|\mathbf{X}_{n,t} - \mathbf{U}_{n,t}\|^2 - \|\mathbf{X}_{n,t+1} - \mathbf{U}_{n,t}\|^2}{2\eta_n} \\
&\stackrel{(c)}{\leq} K_n \left(\sum_{m \in \mathcal{W}_n} G_m \right) \frac{\eta_n}{2} \\
&\quad + \frac{\|\mathbf{X}_{n,t} - \mathbf{U}_{n,t}\|^2 - \|\mathbf{X}_{n,t+1} - \mathbf{U}_{n,t}\|^2}{2\eta_n}, \tag{A-2}
\end{aligned}$$

where (a) follows from Jensen's inequality, (b) from the bounded gradient assumption, and (c) from the definition of K_n .

APPENDIX B PROOF OF THEOREM 4

It follows

$$\begin{aligned}
& \sum_{t=\tau_{n,\min}+1}^{T+\tau_{n,\max}} \frac{\|\mathbf{X}_{n,t} - \mathbf{U}_{n,t}\|^2 - \|\mathbf{X}_{n,t+1} - \mathbf{U}_{n,t}\|^2}{2\eta_n} \\
&= \sum_{t=\tau_{n,\min}+1}^{T+\tau_{n,\max}} \frac{\|\mathbf{X}_{n,t}\|^2 - \|\mathbf{X}_{n,t+1}\|^2}{2\eta_n} \\
&\quad + \sum_{t=\tau_{n,\min}+1}^{T+\tau_{n,\max}} \frac{\langle \mathbf{U}_{n,t}, \mathbf{X}_{n,t+1} \rangle - \langle \mathbf{U}_{n,t}, \mathbf{X}_{n,t} \rangle}{\eta_n} \tag{B-1}
\end{aligned}$$

For the first term in (B-1), we have

$$\begin{aligned}
& \sum_{t=\tau_{n,\min}+1}^{T+\tau_{n,\max}} \frac{\|\mathbf{X}_{n,t}\|^2 - \|\mathbf{X}_{n,t+1}\|^2}{2\eta_n} \\
&= \frac{\|\mathbf{X}_{n,\tau_{n,\min}+1}\|^2}{2\eta_n} - \frac{\|\mathbf{X}_{n,T+\tau_{n,\max}+1}\|^2}{2\eta_n} \\
&\leq \frac{B^2}{2\eta_n}. \tag{B-2}
\end{aligned}$$

For the second term in (B-1), we have

$$\begin{aligned}
& \sum_{t=\tau_{n,\min}+1}^{T+\tau_{n,\max}} \frac{\langle \mathbf{U}_{n,t}, \mathbf{X}_{n,t+1} \rangle - \langle \mathbf{U}_{n,t}, \mathbf{X}_{n,t} \rangle}{\eta_n} \\
&= \sum_{t=\tau_{n,\min}+2}^{T+\tau_{n,\max}} \frac{\langle \mathbf{U}_{n,t-1} - \mathbf{U}_{n,t}, \mathbf{X}_{n,t} \rangle}{\eta_n} \\
&\quad + \frac{\langle \mathbf{U}_{n,T+\tau_{n,\max}}, \mathbf{X}_{n,T+\tau_{n,\max}+1} \rangle}{\eta_n} \\
&\quad - \frac{\langle \mathbf{U}_{n,\tau_{n,\min}+1}, \mathbf{X}_{n,\tau_{n,\min}+1} \rangle}{\eta_n} \\
&\leq B \frac{\sum_{t=\tau_{n,\min}+2}^{T+\tau_{n,\max}} \|\mathbf{U}_{n,t-1} - \mathbf{U}_{n,t}\|}{\eta_n} + \frac{B^2}{4\eta_n} + \frac{B^2}{\eta_n} \\
&\leq \frac{B}{\eta_n} \text{PL}_n^{T+\tau_{n,\max}} + \frac{5B^2}{4\eta_n}, \tag{B-3}
\end{aligned}$$

with the first inequality in (B-3) following from $-B^2/4 \leq \langle \mathbf{X}, \mathbf{Y} \rangle \leq B^2$ [23, Appendix A].

Combining the above results completes the proof.

APPENDIX C PROOF OF BOUND ON $\text{Drift}_{\mathbf{X}}$

Unrolling the difference $\mathbf{X}_{n,t} - \mathbf{X}_{n,t-\tau_{n,m}}$ for $t > \tau_{n,m}$ and from the update rule (14), it holds

$$\begin{aligned}
 & \|\mathbf{X}_{n,t} - \mathbf{X}_{n,t-\tau_{n,m}}\| \tag{C-1} \\
 &= \left\| \sum_{j=1}^{\tau_{n,m}} (\mathbf{X}_{n,t-j+1} - \mathbf{X}_{n,t-j}) \right\| \\
 &\stackrel{(a)}{\leq} \sum_{j=1}^{\tau_{n,m}} \|\mathbf{X}_{n,t-j+1} - \mathbf{X}_{n,t-j}\| \\
 &\stackrel{(b)}{\leq} \eta_n \sum_{j=1}^{\tau_{n,m}} \left\| \sum_{s \in \mathcal{W}_n} w_{n,s} \mathbf{G}_{s,t-j-\tau_{n,s}}^n \mathbb{1}_{\{t-j > \tau_{n,s}\}} \right\| \\
 &\stackrel{(c)}{\leq} \eta_n \sum_{j=1}^{\tau_{n,m}} \sum_{s \in \mathcal{W}_n} w_{n,s} \left\| \mathbf{G}_{s,t-j-\tau_{n,s}}^n \right\| \mathbb{1}_{\{t-j > \tau_{n,s}\}} \\
 &\stackrel{(d)}{\leq} \eta_n \sum_{s \in \mathcal{W}_n} \sum_{j=1}^{\min\{\tau_{n,m}, t-\tau_{n,s}-1\}} w_{n,s} G_s \\
 &\stackrel{(e)}{\leq} \eta_n K_n \sum_{s \in \mathcal{W}_n} \min\{\tau_{n,m}, t-\tau_{n,s}-1\}, \tag{C-2}
 \end{aligned}$$

where (a) and (c) hold by the triangle inequality, (b) follows from $\|\Pi_{\mathcal{X}}[\mathbf{X}] - \mathbf{Y}\|^2 \leq \|\mathbf{X} - \mathbf{Y}\|^2$ for $\mathbf{Y} \in \mathcal{X}$ [7, Proposition 2.11], (d) holds by the bounded gradient assumption, and (e) follows from $\sum_{j=1}^{\min\{a,b\}} c = \min\{a,b\} \times c$, with c being a constant independent of j .

Substituting (34) into (C-2) gives

$$\begin{aligned}
 & \text{Drift}_{\mathbf{X}} \\
 &\leq \sum_{m \in \mathcal{W}_n} K_n^2 \eta_n \sum_{t=\tau_{n,m}+1}^{T+\tau_{n,m}} \sum_{s \in \mathcal{W}_n} \min\{\tau_{n,m}, t-\tau_{n,s}-1\} \\
 &\leq \sum_{t=\tau_{n,\min}+1}^{T+\tau_{n,\max}} K_n^2 \eta_n \sum_{m \in \mathcal{W}_n} \sum_{s \in \mathcal{W}_n} \min\{\tau_{n,m}, t-\tau_{n,s}-1\} \mathbb{1}_{\{t > \tau_{n,m}\}} \\
 &= \sum_{m \in \mathcal{W}_n} \sum_{s \in \mathcal{W}_n} \sum_{t=\tau_{n,m}+1}^{\tau_{n,s}+\tau_{n,m}} K_n^2 \eta_n (t-\tau_{n,s}-1) \\
 &\quad + \sum_{m \in \mathcal{W}_n} \sum_{s \in \mathcal{W}_n} \sum_{t=\tau_{n,s}+\tau_{n,m}+1}^{T+\tau_{n,\max}} K_n^2 \eta_n \tau_{n,m} \\
 &= \sum_{m \in \mathcal{W}_n} \eta_n K_n^2 \sum_{s \in \mathcal{W}_n} \sum_{t=\tau_{n,m}+1}^{\tau_{n,s}+\tau_{n,m}} (t-\tau_{n,s}-1) \\
 &\quad + \sum_{m \in \mathcal{W}_n} \tau_{n,m} K_n^2 \sum_{s \in \mathcal{W}_n} \sum_{t=\tau_{n,s}+\tau_{n,m}+1}^{T+\tau_{n,\max}} \eta_n. \tag{C-3}
 \end{aligned}$$

For the first term in the right side of (C-3), we have

$$\begin{aligned}
 & \sum_{s \in \mathcal{W}_n} \sum_{t=\tau_{n,m}+1}^{\tau_{n,s}+\tau_{n,m}} (t-\tau_{n,s}-1) \\
 &= \sum_{s \in \mathcal{W}_n} \frac{2\tau_{n,m} - \tau_{n,s} - 1}{2} \tau_{n,s} \tag{C-4} \\
 &\leq |\mathcal{W}_n| \tau_{n,\max}^2.
 \end{aligned}$$

For the second term in the right side of (C-3), we have

$$\begin{aligned}
 & \sum_{s \in \mathcal{W}_n} \sum_{t=\tau_{n,s}+\tau_{n,m}+1}^{T+\tau_{n,\max}} \eta_n \leq \sum_{s \in \mathcal{W}_n} \sum_{t=\tau_{n,\min}}^{T+\tau_{n,\max}} \eta_n \\
 &= |\mathcal{W}_n| \sum_{t=\tau_{n,\min}+1}^{T+\tau_{n,\max}} \eta_n \tag{C-5} \\
 &= |\mathcal{W}_n| \eta_n (T + \Delta \tau_n).
 \end{aligned}$$

Combining the above results, we complete this proof.

APPENDIX D PROOF OF LEMMA 2

By unfolding the difference $\mathbf{U}_{n,t} - \mathbf{U}_{n,t-\tau_{n,m}}$, we obtain

$$\begin{aligned}
 & \sum_{t=\tau_{n,m}+1}^{T+\tau_{n,m}} \|\mathbf{U}_{n,t} - \mathbf{U}_{n,t-\tau_{n,m}}\| \\
 &= \sum_{t=\tau_{n,m}+1}^{T+\tau_{n,m}} \left\| \sum_{s=1}^{\tau_{n,m}} (\mathbf{U}_{n,t-s+1} - \mathbf{U}_{n,t-s}) \right\| \\
 &\leq \sum_{t=\tau_{n,m}+1}^{T+\tau_{n,m}} \sum_{s=1}^{\tau_{n,m}} \|\mathbf{U}_{n,t-s+1} - \mathbf{U}_{n,t-s}\| \\
 &= \sum_{t=2}^{T+\tau_{n,m}} \xi_{n,m}^t \|\mathbf{U}_{n,t} - \mathbf{U}_{n,t-1}\|, \tag{D-1}
 \end{aligned}$$

where

$$\xi_{n,m}^t = \begin{cases} t-1, & 2 \leq t \leq \tau_{n,m} \\ \tau_{n,m}, & \tau_{n,m} < t < T \\ T + \tau_{n,m} - t + 1, & T \leq t \leq T + \tau_{n,m} \end{cases}. \tag{D-2}$$

Since $\xi_{n,m}^t \leq \tau_{n,m}$ for all t , we complete this proof.

APPENDIX E COMBINATORIAL OPTIMIZATION-BASED TREE DESIGN

Building on the above design principles, we formulate an optimization problem tailored to our specific design objectives. This formulation is grounded in a flow-conservation-based approach, which accurately models the connectivity requirements and the path-dependent cost characteristics described below:

$$\begin{aligned}
 & \min_{\substack{h_{i,j} \in \{0,1\}, v_i \in \{0,1\} \\ C_{i,j}^w \geq 0, C_{i,j}^{\text{conn}} \geq 0}} \text{Dist} = \sum_{w \in \mathcal{W}_n} \sum_{(i,j) \in \mathcal{E}} \tau_{i,j} (C_{i,j}^w + C_{j,i}^w) \tag{E-1a}
 \end{aligned}$$

$$\text{s.t. } v_w = 1, \quad \forall w \in \mathcal{W}_n \tag{E-1b}$$

$$\sum_{(i,j) \in \mathcal{E}} h_{i,j} = \sum_{i \in \mathcal{N}} v_i - 1 \tag{E-1c}$$

$$h_{i,j} \leq v_i, \quad h_{i,j} \leq v_j, \quad \forall (i,j) \in \mathcal{E} \quad (\text{E-1d})$$

$$C_{i,j}^w + C_{j,i}^w \leq h_{i,j}, \quad \forall w \in \mathcal{W}_n \setminus \{n\}, \quad \forall (i,j) \in \mathcal{E} \quad (\text{E-1e})$$

$$\sum_{j:(n,j) \in \mathcal{E}} C_{n,j}^w - \sum_{j:(j,n) \in \mathcal{E}} C_{j,n}^w = 1, \quad \forall w \in \mathcal{W}_n \setminus \{n\} \quad (\text{E-1f})$$

$$\sum_{j:(w,j) \in \mathcal{E}} C_{w,j}^w - \sum_{j:(j,w) \in \mathcal{E}} C_{j,w}^w = -1, \quad \forall w \in \mathcal{W}_n \setminus \{n\} \quad (\text{E-1g})$$

$$\sum_{j:(i,j) \in \mathcal{E}} C_{i,j}^w - \sum_{j:(j,i) \in \mathcal{E}} C_{j,i}^w = 0, \quad \forall w \in \mathcal{W}_n \setminus \{n\}, \quad \forall i \notin \{n, w\} \quad (\text{E-1h})$$

$$\sum_{j:(n,j) \in \mathcal{E}} C_{n,j}^{\text{conn}} - \sum_{j:(j,n) \in \mathcal{E}} C_{j,n}^{\text{conn}} = \sum_{i \in \mathcal{N}} v_i - 1 \quad (\text{E-1i})$$

$$\sum_{j:(j,i) \in \mathcal{E}} C_{j,i}^{\text{conn}} - \sum_{j:(i,j) \in \mathcal{E}} C_{i,j}^{\text{conn}} = v_i, \quad \forall i \in \mathcal{N} \setminus \{n\} \quad (\text{E-1j})$$

$$C_{i,j}^{\text{conn}} \leq |\mathcal{N}| \cdot h_{i,j}, \quad C_{j,i}^{\text{conn}} \leq |\mathcal{N}| \cdot h_{i,j}, \quad \forall (i,j) \in \mathcal{E} \quad (\text{E-1k})$$

where binary variable $h_{i,j}$ indicates whether edge (i,j) is selected in the resulting tree, and v_i indicates whether node i is included. The auxiliary flow variable $C_{i,j}^w$ captures the unit-demand routing from the root node n to each target node $w \in \mathcal{W}_n$ and contributes to the cost function in (E-1a). Constraints (E-1b)–(E-1e) enforce the tree structure and edge-node consistency. Flow conservation for each demand is captured in (E-1f)–(E-1h). To ensure global connectivity of the tree, an auxiliary flow variable $C_{i,j}^{\text{conn}}$ is introduced. This variable simulates pushing $\sum_{i \in \mathcal{N}} v_i - 1$ units of flow from the root to all active nodes. Constraint (E-1i) initiates the global flow from the root, (E-1j) ensures each activated node receives exactly one unit of flow, and (E-1k) restricts global flow to edges that are less than predefined threshold $|\mathcal{G}|$, which guarantees that all activated nodes are connected within a single tree structure.

This problem (E-1) is formulated as a mixed integer programming problem, which can be solved by existing solvers, like PuLP, and Gurobi.

REFERENCES

- [1] B. Wang, M. Zecchin, and O. Simeone, “Distributed associative memory via online convex optimization,” *arXiv preprint arXiv:2509.22321*, 2025.
- [2] E. Tulving *et al.*, “Episodic and semantic memory,” *Organization of memory*, vol. 1, no. 381-403, p. 1, 1972.
- [3] A. Vaswani, N. Shazeer, N. Parmar, J. Uszkoreit, L. Jones, A. N. Gomez, Ł. Kaiser, and I. Polosukhin, “Attention is all you need,” *Proc. Adv. Neural Inf. Process. Syst.*, vol. 30, 2017.
- [4] A. Behrouz, M. Razaviyayn, P. Zhong, and V. Mirrokni, “It’s all connected: A journey through test-time memorization, attentional bias, retention, and online optimization,” *arXiv preprint arXiv:2504.13173*, 2025.
- [5] K. A. Wang, J. Shi, and E. B. Fox, “Test-time regression: a unifying framework for designing sequence models with associative memory,” *arXiv preprint arXiv:2501.12352*, 2025.
- [6] S. Zhong, M. Xu, T. Ao, and G. Shi, “Understanding transformer from the perspective of associative memory,” *arXiv preprint arXiv:2505.19488*, 2025.
- [7] F. Orabona, “A modern introduction to online learning,” *arXiv preprint arXiv:1912.13213*, 2019.
- [8] S. Shalev-Shwartz *et al.*, “Online learning and online convex optimization,” *Found. Trends Mach. Learn.*, vol. 4, no. 2, pp. 107–194, 2012.
- [9] S. Gezici, Z. Tian, G. B. Giannakis, H. Kobayashi, A. F. Molisch, H. V. Poor, and Z. Sahinoglu, “Localization via ultra-wideband radios: a look at positioning aspects for future sensor networks,” *IEEE Signal Process. Mag.*, vol. 22, no. 4, pp. 70–84, 2005.
- [10] F. Hussain, S. A. Hassan, R. Hussain, and E. Hossain, “Machine learning for resource management in cellular and IoT networks: Potentials, current solutions, and open challenges,” *IEEE Commun. Surveys Tuts.*, vol. 22, no. 2, pp. 1251–1275, 2020.
- [11] P. Popovski, K. F. Trillingsgaard, O. Simeone, and G. Durisi, “5G wireless network slicing for eMBB, URLLC, and mMTC: A communication-theoretic view,” *IEEE Access*, vol. 6, pp. 55 765–55 779, 2018.
- [12] M. Rabbat and R. Nowak, “Distributed optimization in sensor networks,” in *Proc. 3rd Int. Symp. Inf. Process. Sensor Netw.*, 2004, pp. 20–27.
- [13] J. D. Hamilton, *Time series analysis*. Princeton university press, 2020.
- [14] S. P. Sone, J. J. Lehtomäki, and Z. Khan, “Wireless traffic usage forecasting using real enterprise network data: Analysis and methods,” *IEEE Open J. Commun. Soc.*, vol. 1, pp. 777–797, 2020.
- [15] J. J. Hopfield, “Neural networks and physical systems with emergent collective computational abilities,” *Proc. of the National Academy of Sciences*, vol. 79, no. 8, pp. 2554–2558, 1982.
- [16] D. Krotov and J. J. Hopfield, “Dense associative memory for pattern recognition,” *Proc. Adv. Neural Inf. Process. Syst.*, vol. 29, 2016.
- [17] D. Krotov and J. Hopfield, “Large associative memory problem in neurobiology and machine learning, arxiv,” *arXiv preprint arXiv:2008.06996*, 2020.
- [18] H. Ramsauer, B. Schäfl, J. Lehner, P. Seidl, M. Widrich, T. Adler, L. Gruber, M. Holzleitner, M. Pavlović, G. K. Sandve *et al.*, “Hopfield networks is all you need,” *arXiv preprint arXiv:2008.02217*, 2020.
- [19] A. Katharopoulos, A. Vyas, N. Pappas, and F. Fleuret, “Transformers are RNNs: Fast autoregressive transformers with linear attention,” in *Proc. Int. Conf. Mach. Learn.*, Virtual Site, 2020, pp. 5156–5165.
- [20] S. Yang, B. Wang, Y. Shen, R. Panda, and Y. Kim, “Gated linear attention transformers with hardware-efficient training,” *arXiv preprint arXiv:2312.06635*, 2023.
- [21] I. Schlag, K. Irie, and J. Schmidhuber, “Linear transformers are secretly fast weight programmers,” in *Proc. Int. Conf. Mach. Learn.*, Virtual Site, 2021, pp. 9355–9366.
- [22] Z. Lin, E. Nikishin, X. O. He, and A. Courville, “Forgetting transformer: Softmax attention with a forget gate,” *arXiv preprint arXiv:2503.02130*, 2025.
- [23] M. Zinkevich, “Online convex programming and generalized infinitesimal gradient ascent,” in *Proc. Int. Conf. Mach. Learn.*, Washington, DC, USA, 2003, pp. 928–936.
- [24] T. Yang, L. Zhang, R. Jin, and J. Yi, “Tracking slowly moving clairvoyant: Optimal dynamic regret of online learning with true and noisy gradient,” in *Proc. Int. Conf. Mach. Learn.*, New York, NY, USA, 2016, pp. 449–457.
- [25] P. Zhao, Y.-J. Zhang, L. Zhang, and Z.-H. Zhou, “Dynamic regret of convex and smooth functions,” *Proc. Adv. Neural Inf. Process. Syst.*, vol. 33, pp. 12 510–12 520, 2020.
- [26] L. Zhang, T.-Y. Liu, and Z.-H. Zhou, “Adaptive regret of convex and smooth functions,” in *Proc. Int. Conf. Mach. Learn.*, California, USA, 2019, pp. 7414–7423.
- [27] X. Cao, T. Başar, S. Diggavi, Y. C. Eldar, K. B. Letaief, H. V. Poor, and J. Zhang, “Communication-efficient distributed learning: An overview,” *IEEE J. Sel. Areas Commun.*, vol. 41, no. 4, pp. 851–873, 2023.
- [28] P. Kairouz, H. B. McMahan, B. Avent, A. Bellet, A. N. Bhagoji, K. Bonawitz, Z. Charles, G. Cormode, R. Cummings *et al.*, “Advances and open problems in federated learning,” *Found. Trends Mach. Learn.*, vol. 14, no. 1–2, pp. 1–210, 2021.
- [29] R. Xin, S. Pu, A. Nedić, and U. A. Khan, “A general framework for decentralized optimization with first-order methods,” *Proc. IEEE*, vol. 108, no. 11, pp. 1869–1889, 2020.
- [30] A. G. Dimakis, S. Kar, J. M. Moura, M. G. Rabbat, and A. Scaglione, “Gossip algorithms for distributed signal processing,” *Proc. IEEE*, vol. 98, no. 11, pp. 1847–1864, 2010.
- [31] Y. Zhang and Q. Yang, “A survey on multi-task learning,” *IEEE Trans. Knowl. Data Eng.*, vol. 34, no. 12, pp. 5586–5609, 2021.
- [32] S. Liu, S. J. Pan, and Q. Ho, “Distributed multi-task relationship learning,” in *Proc. ACM SIGKDD Int. Conf. Knowl. Discov. Data Min.*, Halifax, NS, Canada, 2017, pp. 937–946.
- [33] R. Nassif, S. Vlaski, C. Richard, J. Chen, and A. H. Sayed, “Multitask learning over graphs: An approach for distributed, streaming machine learning,” *IEEE Signal Process. Mag.*, vol. 37, no. 3, pp. 14–25, 2020.
- [34] F. Yan, S. Sundaram, S. Vishwanathan, and Y. Qi, “Distributed autonomous online learning: Regrets and intrinsic privacy-preserving properties,” *IEEE Trans. Knowl. Data Eng.*, vol. 25, no. 11, pp. 2483–2493, 2013.
- [35] F. Orabona and D. Pál, “Coin betting and parameter-free online learning,” *Proc. Adv. Neural Inf. Process. Syst.*, vol. 29, 2016.